# Article

# Age-specific mortality and immunity patterns of SARS-CoV-2

Megan O'Driscoll[1,2 ✉], Gabriel Ribeiro Dos Santos[1,2], Lin Wang[1,2], Derek A. T. Cummings[3], Andrew S. Azman[4,5], Juliette Paireau[2,6], Arnaud Fontanet[6,7], Simon Cauchemez[2,8 ✉] & Henrik Salje[1,2,8 ✉]

Estimating the size of the coronavirus disease 2019 (COVID-19) pandemic and the infection severity of severe acute respiratory syndrome coronavirus 2 (SARS-CoV-2) is made challenging by inconsistencies in the available data. The number of deaths associated with COVID-19 is often used as a key indicator for the size of the epidemic, but the observed number of deaths represents only a minority of all infections[1,2]. In addition, the heterogeneous burdens in nursing homes and the variable reporting of deaths of older individuals can hinder direct comparisons of mortality rates and the underlying levels of transmission across countries[3]. Here we use age-specific COVID-19-associated death data from 45 countries and the results of 22 seroprevalence studies to investigate the consistency of infection and fatality patterns across multiple countries. We find that the age distribution of deaths in younger age groups (less than 65 years of age) is very consistent across different settings and demonstrate how these data can provide robust estimates of the share of the population that has been infected. We estimate that the infection fatality ratio is lowest among 5–9-year-old children, with a log-linear increase by age among individuals older than 30 years. Population age structures and heterogeneous burdens in nursing homes explain some but not all of the heterogeneity between countries in infection fatality ratios. Among the 45 countries included in our analysis, we estimate that approximately 5% of these populations had been infected by 1 September 2020, and that much higher transmission rates have probably occurred in a number of Latin American countries. This simple modelling framework can help countries to assess the progression of the pandemic and can be applied in any scenario for which reliable age-specific death data are available.

As SARS-CoV-2 continues its rapid global spread, increased understanding of the underlying level of transmission and infection severity are crucial for guiding the pandemic response. Although the testing of individuals with COVID-19 is a vital public health tool, variability in surveillance capacities, case definitions and health-seeking behaviour can cause difficulties in the interpretation of case data. Owing to more complete reporting, COVID-19-associated deaths are often seen as a more reliable indicator of the size of the pandemic. If reliably reported, the number of COVID-19-associated deaths can be used to infer the total number of SARS-CoV-2 infections using estimates of the infection fatality ratio (IFR; the ratio of COVID-19-associated deaths to the total number of SARS-CoV-2 infections). Estimates of the IFR derived from seroprevalence studies that carefully estimate the number of individuals with detectable antibodies can help to make the link between deaths and total infections as well as refine estimates of the relative burden in different age groups[1]. Although it is clear that

infection severity increases substantially with age[2,4], there remain key unanswered questions with regard to the consistency of mortality patterns across countries. Underlying heterogeneities in the age structure of the population or in the prevalence of comorbidities can contribute to differences in the levels of observed COVID-19-associated fatalities[5]. In addition, when looking at the total number of COVID-19-associated deaths, the level of transmission among the general population can be difficult to disentangle from large outbreaks in vulnerable populations such as those living in nursing homes and other long-term care settings. For many countries, the COVID-19 pandemic has been characterized by a heavy burden in residents of nursing homes, with more than 20% of all reported COVID-19-associated deaths occurring in nursing homes in countries such as Canada, Sweden and the UK[3]. In other countries, such as South Korea and Singapore, few COVID-19-associated deaths have been reported in nursing homes[3]. In this context, simply comparing the total number of deaths across countries may provide

[1]Department of Genetics, University of Cambridge, Cambridge, UK. [2]Mathematical Modelling of Infectious Diseases Unit, Institut Pasteur, UMR2000, CNRS, Paris, France. [3]Department of Biology and Emerging Pathogens Institute, University of Florida, Gainesville, FL, USA. [4]Department of Epidemiology, Johns Hopkins Bloomberg School of Public Health, Baltimore, MD, USA. [5]Unit of Population Epidemiology, Division of Primary Care Medicine, Geneva University Hospitals, Geneva, Switzerland. [6]Emerging Infectious Diseases Unit, Institut Pasteur, Paris, France. [7]PACRI Unit, Conservatoire National des Arts et Métiers, Paris, France. [8]These authors jointly supervised this work: Simon Cauchemez, Henrik Salje. ✉e-mail: mo487@cam.ac.uk; simon.cauchemez@pasteur.fr; hs743@cam.ac.uk
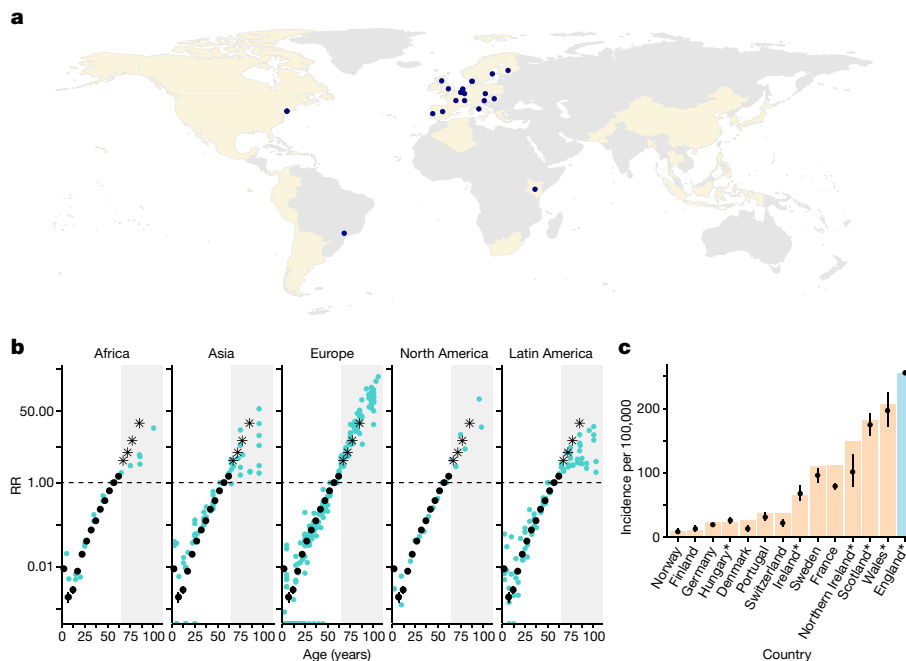
**Fig. 1 | Patterns of COVID-19-associated mortality across settings.**
**a**, Countries with age-specific death data (beige) and locations with
seroprevalence data (dots). **b**, Estimated median and 95% credible intervals of
the proportion of the population that has died in each age group, relative to the
proportion of population that has died among 55–59-year-old individuals in
that country (black dots and lines), plotted on a log-linear scale. Coloured dots
represent the country- and age-specific relative risks (RR) of COVID-
19-associated death in the population relative to the risks of 55–59-year-old
individuals observed from reported death data, accounting for population age
distributions (Supplementary Methods 1) ($n$ = 538,477 reported deaths). All
data points are plotted at the midpoint of the reported age group. The grey
shaded areas highlight the relative risks of death by age for age groups of

65 years and older, which were excluded from model fitting and black asterisks
represent estimates inferred solely from England data, which were derived
independent of deaths that occurred in nursing homes. **c**, Comparing the
reconstructed incidence of deaths with reported data for age groups aged 60
or 65 years and older for a subset of countries from which deaths that occurred
in nursing homes could be excluded. Black dots and lines indicate the
estimated median and 95% credible intervals derived from only the England
data (blue bar); orange bars show the reported incidence of deaths of
individuals aged 60 years and older in 13 additional countries that did not occur
in nursing homes. Countries labelled with an asterisk indicate those in which
the number of deaths were reconstructed for those aged 65 years and older, to
align with the reported age groups for each country.

a misleading representation of the underlying level of transmission.
Focusing on COVID-19-associated death data in younger individuals,
however, may provide more-reliable insights into the underlying nature
of transmission.

Seroprevalence surveys provide valuable information on the pro-
portion of the population that have ever experienced an infection[6–9],
however, they can be subject to a number of biases and variable per-
formance of different assays can complicate comparisons of results
across studies[10]. Here, we present a model framework that integrates
age-specific COVID-19-associated death data from 45 countries with
22 national-level seroprevalence surveys, providing insights into the
consistency of infection fatality patterns across countries (Fig. 1a). We
use our model to produce ensemble IFR estimates by age and sex in a
single harmonized framework as well as estimates of the proportion
of the population that has been infected in each country.

## Age-specific mortality patterns

Using population age structures and age-specific death data, we com-
pare the relative number of deaths by age within each country, using
55–59-year-old individuals as the reference group. We find a very con-
sistent pattern in the relative risk of death by age for individuals younger
than 65 years of age across countries and continents, with a strong
log-linear relationship between age and risk of death for individuals
who are 30–65 years old (Fig. 1b and Supplementary Methods 1). The
observed relative risk of death in older individuals appears to be sub-
stantially more heterogeneous across locations. Given the potential for
important variability in mortality associated with outbreaks in nursing

homes across countries, we first investigate mortality patterns specifi-
cally in the general population, using age-specific deaths of individuals
aged 65 years and older from England, for which the granularity of
the data enables us to remove deaths that occurred in nursing home
populations. We find that the log-linear relationship between age and
risk of death continues into older age groups (Fig. 1b). To assess the
generalizability of the data from England to other countries, we use
these estimates to reconstruct the number of deaths in the general
population—that is, excluding nursing homes—in 13 other countries
and find that the predictions are consistent with the reported num-
bers of deaths in the general population (Fig. 1c and Supplementary
Methods 2).

To translate the relative risks of death by age to the underlying IFR,
we combine age-specific death data with 22 seroprevalence surveys,
representing 16 of the 45 countries (multiple studies are available
for Belgium, England, Scotland, Sweden and the Netherlands) (Sup-
plementary Table 1). We use daily time series of reported deaths to
reconstruct the timing of infections and subsequent seroconversions.
To limit biases that can be introduced by outbreaks in nursing homes
and potentially variable reporting practices of fatalities among indi-
viduals aged 65 years of age and older, we fit our model investigating
the relationship between seroconversion and mortality exclusively
to death data from those younger than 65 years. To infer IFRs in age
groups 65 years and older, we use our estimates of the relative risk of
death derived from data from England of deaths that did not occur in
nursing homes. As our baseline model, we use an ensemble model in
which we include results from all national-level seroprevalence studies
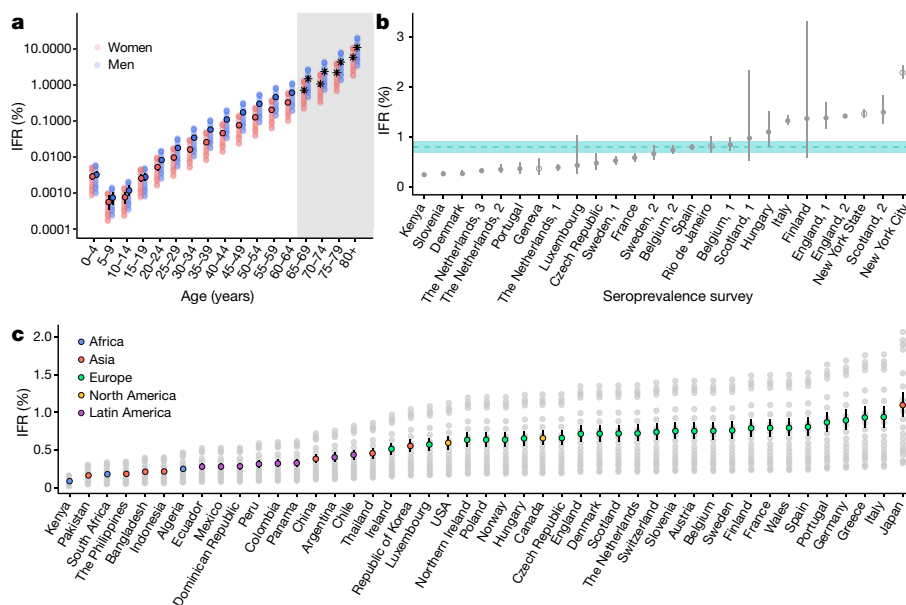within a single framework. In addition, we consider separate models

**Fig. 2 | IFR estimates. a**, Estimated median and 95% credible intervals of the IFR, stratified by age and sex and plotted on a log-linear scale. The IFR is estimated with the ensemble model (filled dots and black lines). Black asterisks on the right represent the estimated IFRs for age groups of 65 years and older, which were excluded from the fitting of the ensemble model. The semi-transparent dots represent median IFRs estimated from separately fitting the model to each individual seroprevalence survey. **b**, Population-weighted IFR estimates derived from separately fitting individual seroprevalence surveys in the model and using France as a reference population, with points and lines indicating the median and 95% credible intervals. The blue dashed line and ribbon indicate the median and 95% credible intervals of the population-weighted IFR produced by the ensemble model. Hollow dots represent the estimates from subnational seroprevalence surveys that were excluded from the fitting of the ensemble model. **c**, Median and 95% credible intervals of the population-weighted IFRs estimated by the ensemble model for each of the 45 countries, coloured by continent. Grey dots represent the median estimates for each country, derived from fitting the model separately to each individual seroprevalence survey.

for which we use the results of each individual seroprevalence survey to investigate the consistency of estimates provided by different studies. As older individuals have fewer social contacts[11] and are more likely to be isolated through shielding programmes, we assume a baseline relative infection attack rate of 0.7 for individuals aged 65 years and older, relative to those under 65, and assume equal infection attack rates across age groups under 65 years of age. We find that age-specific IFRs estimated by the ensemble model range from 0.001% (95% credible interval, 0–0.001) in those aged 5–9 years old (range, 0–0.002% across individual national-level seroprevalence surveys) to 8.29% (95% credible intervals, 7.11–9.59%) in those aged 80+ (range, 2.49–15.55% across individual national-level seroprevalence surveys) (Fig. 2a). We estimate a mean increase in IFR of 0.59% with each five-year increase in age (95% credible interval, 0.51–0.68%) for ages of 10 years and older. We estimate that the risk of death if infected with SARS-CoV-2 is significantly higher for men than for women (Fig. 2a) particularly in older individuals with ensemble IFR estimates of 10.83% for men aged 80+ (95% credible interval, 9.28–12.52%; range of each individual seroprevalence survey, 3.25–20.30%) and 5.76% for women aged 80+ (95% credible interval, 4.94–6.66%; individual seroprevalence survey range, 1.73–10.80%), which is consistent with previous findings[12,13].

## Consistency of IFRs across seroprevalence surveys

We use our model framework to facilitate robust comparisons of IFRs across settings, considering only age-specific deaths among those younger than 65 years old. Using country-specific demographic distributions (both age and sex), we estimate population-weighted IFRs for each country. Taking France as a reference population, the ensemble model estimates a population IFR of 0.79% (95% credible interval, 0.68–0.92%), although we find notable heterogeneity in IFR estimates

as suggested by individual national-level seroprevalence studies, with a median range of 0.24–1.49% (Fig. 2b). In particular, seroprevalence studies from New York City (2.28; 95% credible interval, 2.15–2.42%), Scotland (1.49%; 95% credible interval, 1.25–1.82%) and England (1.41%; 95% credible intervals, 1.38–1.44%) suggest a significantly higher IFR whereas studies in Kenya (0.24%; 95% credible interval, 0.23–0.25%), Slovenia (0.25%; 95% credible interval, 0.24–0.30%) and Denmark (0.26%; 95% credible interval, 0.24–0.32%) support a lower IFR than that of the ensemble model. We note that the application of age- and sex-specific IFR estimates suggested by individual national-level sero-prevalence studies at the lower end of the scale (for example, Kenya, Slovenia and Denmark) to mortality data in highly affected settings would suggest attack rates over 100% (Supplementary Fig. 3). Potential explanations for the variable IFR estimates observed across settings include different prevalences of high-risk populations (for example, individuals with comorbidities), differences in methodology and representativeness of seroprevalence studies, heterogeneities in availability and quality of care or variations in reporting of COVID-19-associated deaths. We have fitted our model to seroprevalence data adjusted for reported assay sensitivity and specificity but find that using unadjusted estimates provides similar results (Supplementary Fig. 5). As the duration of SARS-CoV-2 seropositivity among infected individuals is as-yet unclear[14], in sensitivity analyses we explore the potential effect of waning antibodies over time. In a scenario with assumed 5% exponential decay of seroconversions per month, the ensemble model estimates a population IFR of 0.65% in France (95% credible interval, 0.56–0.73%) (Supplementary Fig. 4). Furthermore, we demonstrate that our results are robust to different assumptions regarding the mean delay between infection and seroconversion (Supplementary Fig. 4). There may also be individuals who never seroconvert or only develop a T cell response, and those individuals would be missed in these studies[15]. Of the studies
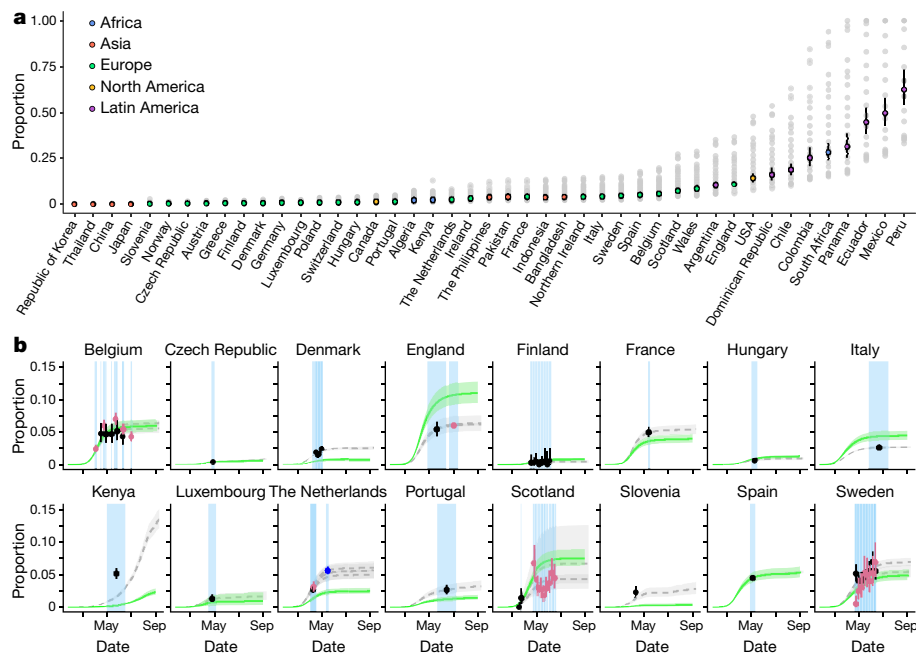
**Fig. 3 | Infection attack rates. a**, Estimates of the infected population proportion for each country as of 1 September 2020. The *y* axis in **a** has been capped at 1, whereas in Supplementary Fig. 4 the same graph is shown with the full range of values. Grey dots indicate the median estimates by fitting the model to each individual seroprevalence survey. Coloured dots and lines represent the median and 95% credible intervals estimated by the ensemble model. **b**, Proportion of the population who are seropositive over time for each of the 12 countries fit with national-level seroprevalence data. Green curves and ribbons indicate the median and 95% credible intervals estimated by the ensemble model. Dots and lines represent the mean and 95% binomial

confidence interval of the published seroprevalence data. For countries with more than 1 seroprevalence survey, black dots and lines correspond to the study that is designated 'country, 1' (for example, Sweden, 1) in Fig. 2 and Supplementary Table 1, whereas pink dots and lines correspond to the study designated 'country, 2' (for example, Belgium, 2) and navy dots and lines to the study designated 'country, 3' (for example, The Netherlands, 3). Blue-shaded regions indicate the start and end dates of sampling for each seroprevalence survey. Grey dashed lines and ribbons represent the median and 95% credible interval model estimates derived from separately fitting the model to each individual seroprevalence study.

included in our analysis, we find that those conducted among blood donors (which exclude children and require individuals to be asymptomatic at the time of sampling) do not give significantly different results to those conducted among the general population (Supplementary Fig. 6). However, further comparisons are needed to fully understand the representativeness of different seroprevalence survey designs.

Considering the demographic structures of each country, we find that population-weighted IFR estimates by the ensemble model are highest for countries with older populations such as Japan (1.09%; 95% credible interval, 0.94–1.26%; individual seroprevalence survey range, 0.33–2.05%) and Italy (0.94%; 95% credible interval, 0.80–1.08%; individual seroprevalence survey range, 0.28–1.76%), whereas the lowest IFRs are for Kenya (0.09%; 95% credible interval, 0.08–0.10%; individual seroprevalence survey range, 0.03–0.17%) and Pakistan (0.16%; 95% credible interval, 0.14–0.19%; individual seroprevalence survey range, 0.05–0.31%) (Fig. 2c). Our ensemble model reproduces the reported seroprevalence values for the majority of studies including the temporal dynamics. However, consistent with substantial heterogeneity in IFR across countries, the ensemble model cannot fully reconcile the relationship between reported seroprevalence and age-specific death data in some locations (Fig. 3b). Of the 45 countries included in our analysis, which represent 3.4 billion people, we estimate that an average of 5.27% (95% credible interval, 4.51–6.20%; individual seroprevalence survey range, 2.80–13.97%) of these populations had been infected by 1 September 2020, ranging from 0.06% (95% credible interval, 0.04–0.09%; individual seroprevalence survey range, 0.02–0.20%) in South Korea to 62.44% (95% credible interval, 54.07–72.90%; individual seroprevalence survey range, 33.13–207.20%) in Peru. These results indicate that there has been large heterogeneity in the level of

transmission across countries to date, with particularly high attack rates estimated in many Latin American countries. Given the underlying heterogeneity in IFR that could not be captured by the ensemble model, it is important to consider the full range of uncertainty in these estimates as suggested by individual seroprevalence studies (grey points in Fig. 3b). Estimates of high transmission levels in some Latin American countries are consistent with recent subnational seroprevalence studies[16–18]. Our estimates are also consistent with mathematical modelling efforts for individual countries, in which additional metrics of epidemic size (for example, numbers of cases, hospitalizations and/or admissions to intensive care units) have been considered[12,19,20] (Supplementary Fig. 7). The medium and longer term implications for the pandemic in countries that have experienced high levels of infection remain unclear; in particular, whether sufficient immunity exists to halt the pandemic locally[21].

## Heterogeneities in mortality in individuals over 65

Using our model framework, we estimate the number of deaths expected in the absence of transmission in nursing homes in those aged 65 years and older, given the reported number of deaths in younger age groups, and compare them to the reported number of COVID-19-associated deaths in individuals aged 65 years and older (Fig. 4a). We find that many countries in Latin America had significantly fewer reported deaths in individuals aged 65 years and older than expected, consistent with the underreporting of COVID-19-associated deaths among older individuals. For example, we find that in Ecuador there are 220 fewer reported deaths per 100,000 individuals in those aged 65 years and older than expected (95% credible interval,
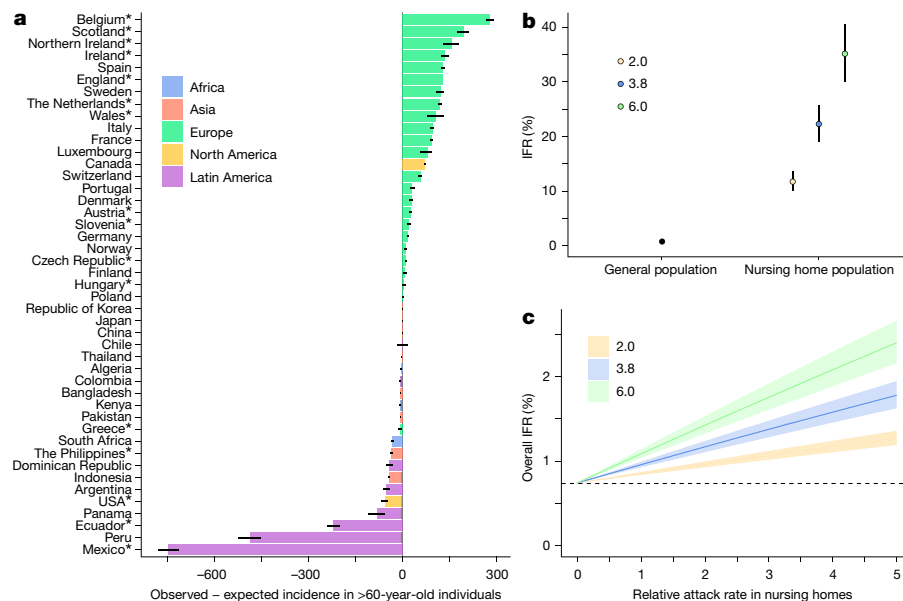
**Fig. 4 | Infection fatality patterns among individuals who are 60 years and older. a**, Difference between the reported and expected incidence of COVID-19-associated deaths per 100,000 individuals in the population among individuals who are ≥60 or ≥65 years of age in each country. Coloured bars represent the median difference and black lines represent 95% credible intervals. Countries labelled with an asterisk indicate those for which the number of deaths was reconstructed for ages 65+ years, to align with the reported age groups for each country (*n* = 429,039 reported deaths 60 or 65+ years of age). **b**, Population-weighted IFRs for the general population and residents of nursing homes, using France as a reference population (*n* = 10,560 reported deaths among residents of nursing homes and *n* = 20,528 among the

general population). The relative frailty of residents of nursing homes is assumed to be 2 (yellow), 3.8 (green) or 6 (blue). Dots and lines indicate the median and 95% credible intervals estimated by the ensemble model. **c**, Population-weighted IFR in France, estimated with different assumed infection attack rates and frailty of residents of nursing homes relative to those of the same age and sex in the general population. Coloured ribbons indicate 95% credible intervals and the black dashed line represents the median population-weighted IFR estimated when assuming a zero infection attack rate among residents of nursing homes (*n* = 10,560 reported deaths among residents of nursing homes and *n* = 20,528 among the general population).

200–240), equivalent to approximately 2,800 missing deaths. Although lower infection attack rates in older populations owing to a reduced number of contacts or successful shielding policies may also explain lower mortality rates, in sensitivity analyses we show that for some countries unrealistically low infection attack rates among individuals aged 65 years and older compared to the rest of the population would be required to reconcile the reported number of deaths in these age groups (Supplementary Fig. 8).

By contrast, for many European countries, we observe a higher incidence of deaths in older individuals than expected (Fig. 4a). This is consistent with the large proportion of reported COVID-19-associated deaths attributable to outbreaks in nursing homes, highlighting the enormous burden experienced by these communities in many higher-income countries[22,23]. We use the age and sex distribution of residents in nursing homes to derive a population-weighted IFR of 22.25% (95% credible interval, 19.06–25.74%) among residents in nursing home in France, assuming that individuals in nursing homes are 3.8 times more frail than individuals in the general population of the same age and sex, as has previously been estimated[24] (Fig. 4b). Using this estimate of the IFR would suggest that 7.28% of the French nursing home population had been infected by 1 September 2020 (95% credible interval, 6.29–8.49%), a 1.70-fold higher infection attack rate than the general population (Supplementary Methods 3). In our baseline model, we derive IFR estimates among the general population (that is, excluding deaths that occurred in nursing homes) so as to facilitate robust comparisons of IFR and transmission in the general population across settings. However, we demonstrate that in cases in which high rates of infection have occurred among residents of nursing homes, overall IFRs will be significantly greater than in scenarios in which these populations have been successfully shielded or experienced little exposure (Fig. 4c). For example, in France, including deaths that occurred in

nursing homes increases the IFR from 0.74% for the general population (95% credible interval, 0.64–0.86%) to 1.10% overall (95% credible interval, 0.95–1.28%). This highlights the complexity of comparing headline IFR estimates across populations in which very different levels of transmission may have occurred in these hyper-vulnerable communities.

## Discussion

In our analysis, we assess the relationship between seroprevalence and the age-specific number of COVID-19-associated deaths across numerous settings. Accounting for population demographics and variable mortality burdens among older populations, we find considerable heterogeneity in the overall IFR of SARS-CoV-2 across settings, which suggests that there are additional important drivers of IFRs.

Seroprevalence surveys have, to date, shown inconsistent patterns in age-specific infection attack rates across settings (Supplementary Fig. 10) as contact patterns are likely to have changed substantially over the course of the pandemic. In sensitivity analyses, we find that our results are relatively consistent when using different assumed age-specific infection attack rates (Supplementary Fig. 9). Here we use data from national reporting systems of COVID-19-associated deaths. However, in some settings these may not capture all deaths associated with COVID-19. It has been estimated for a subset of countries (*n* = 6 out of 45) that the numbers of reported COVID-19-associated deaths ranged between undercounting of 40% to overcounting of 10% compared to excess death estimates[25]. Assuming that these differences occur equally across all age groups would result in a change in the mean IFR for these countries of 0.66% to 0.87%. However, this represents an extreme scenario, as most unaccounted for deaths are likely to be in the oldest age groups, which would not affect our estimates[25]. There are a number of complexities in the interpretation of excess death data that

can inhibit their direct use in assessments of IFR. Specifically, excess death estimates are highly sensitive to the reference time period used (Supplementary Figs. 11, 12), frequent negative excess deaths occur, especially in younger ages (Supplementary Fig. 12), and there is limited availability of excess death data for narrow age groups or outside higher-income countries. Although both seroprevalence and reported COVID-19-associated death data can be subject to potential limitations, considering these data across multiple settings in a harmonized framework has enabled us to robustly assess trends in the transmission and fatality rates of SARS-CoV-2 and derive global ensemble estimates.

Translating the number of COVID-19-associated deaths into estimates of the number of infections requires careful consideration of fatalities from outbreak events in highly vulnerable populations. By providing a benchmark of the expected number of deaths by age in older individuals, our approach allows us to identify countries in which excess transmission in nursing home populations has probably occurred. We demonstrate how outbreaks in nursing homes can drive overall population IFRs, through both increased attack rates and increased vulnerability. The results and modelling framework that we present here demonstrate how age-specific death data can be used to robustly reconstruct the underlying level of transmission. This approach could be applied at subnational scale and may be of particular use in settings in which resources to carry out large, representative seroprevalence studies are not available.

## Online content

Any methods, additional references, Nature Research reporting summaries, source data, extended data, supplementary information, acknowledgements, peer review information; details of author contributions and competing interests; and statements of data and code availability are available at https://doi.org/10.1038/s41586-020-2918-0.

1. Pastor-Barriuso, R. et al. Infection fatality risk for SARS-CoV-2: a nationwide seroepidemiological study in the non-institutionalized population of Spain. Preprint at http://doi.org/10.1101/2020.08.06.20169722 (2020).
2. Verity, R. et al. Estimates of the severity of coronavirus disease 2019: a model-based analysis. *Lancet Infect. Dis.* **20**, 669–677 (2020).
3. Comas-Herrera, A. et al. *Mortality associated with COVID-19 Outbreaks in Care Homes: Early International Evidence*. https://ltccovid.org/2020/04/12/mortality-associated-with-covid-19-outbreaks-in-care-homes-early-international-evidence/ (2020).
4. Guan, W.-J. et al. Clinical characteristics of coronavirus disease 2019 in China. *N. Engl. J. Med.* **382**, 1708–1720 (2020).
5. Clark, A. et al. Global, regional, and national estimates of the population at increased risk of severe COVID-19 due to underlying health conditions in 2020: a modelling study. *Lancet Glob. Health* **8**, e1003–e1017 (2020).
6. Pollán, M. et al. Prevalence of SARS-CoV-2 in Spain (ENE-COVID): a nationwide, population-based seroepidemiological study. *Lancet* **396**, 535–544 (2020).
7. Stringhini, S. et al. Seroprevalence of anti-SARS-CoV-2 IgG antibodies in Geneva, Switzerland (SEROCoV-POP): a population-based study. *Lancet* **396**, 313–319 (2020).
8. Rosenberg, E. S. et al. Cumulative incidence and diagnosis of SARS-CoV-2 infection in New York. *Ann. Epidemiol.* **48**, 23–29 (2020).
9. Herzog, S. et al. Seroprevalence of IgG antibodies against SARS coronavirus 2 in Belgium — a prospective cross-sectional study of residual samples. Preprint at https://doi.org/10.1101/2020.06.08.20125179 (2020).
10. Takahashi, S., Greenhouse, B. & Rodríguez-Barraquer, I. Are seroprevalence estimates for severe acute respiratory syndrome coronavirus 2 biased? *J. Infect. Dis.* **222**, 1772–1775 (2020).
11. Prem, K., Cook, A. R. & Jit, M. Projecting social contact matrices in 152 countries using contact surveys and demographic data. *PLOS Comput. Biol.* **13**, e1005697 (2017).
12. Salje, H. et al. Estimating the burden of SARS-CoV-2 in France. *Science* **369**, 208–211 (2020).
13. Jin, J.-M. et al. Gender differences in patients with COVID-19: focus on severity and mortality. *Front. Public Health* **8**, 152 (2020).
14. Huang, A. T. et al. A systematic review of antibody mediated immunity to coronaviruses: kinetics, correlates of protection, and association with severity. *Nat. Commun.* **11**, 4704 (2020).
15. Braun, J. et al. SARS-CoV-2-reactive T cells in healthy donors and patients with COVID-19. *Nature* **587**, 270–274 (2020).
16. Buss, L. F. et al. COVID-19 herd immunity in the Brazilian Amazon. Preprint at https://doi.org/10.1101/2020.09.16.20194787 (2020).
17. Antonio, C. A. A. et al. *Seroprevalencia de Anticuerpos anti SARS-CoV-2 en la Ciudad de Iquitos, Loreto, Perú.* https://docs.google.com/document/d/1K-aKyFmxztdfNJOtXuSH1uGcBeaZA7LH/edit (2020).
18. Del Brutto, O. H. et al. SARS-CoV-2 in rural Latin America. A population-based study in coastal Ecuador. *Clin. Infect. Dis.* ciaa1055 (2020).
19. Flaxman, S. et al. Estimating the effects of non-pharmaceutical interventions on COVID-19 in Europe. *Nature* **584**, 257–261 (2020).
20. Abrams, S. et al. Modeling the early phase of the Belgian COVID-19 epidemic using a stochastic compartmental model and studying its implied future trajectories. Preprint at https://doi.org/10.1101/2020.06.29.20142851 (2020).
21. Fontanet, A. & Cauchemez, S. COVID-19 herd immunity: where are we? *Nat. Rev. Immunol.* **20**, 583–584 (2020).
22. Molenberghs, G. et al. Belgian COVID-19 mortality, excess deaths, number of deaths per million, and infection fatality rates (8 March - 9 May 2020). Preprint at https://doi.org/10.1101/2020.06.20.20136234 (2020).
23. Soveri, H. et al. Why, in almost all countries, was residential care for older people so badly affected by COVID-19? http://www.ose.be/files/publication/OSEPaperSeries/Declercq_Et_Al_2020_OpinionPaper23.pdf (European Social Observatory, 2020).
24. Hardy, O. J. et al. A world apart: levels and factors of excess mortality due to COVID-19 in care homes. The case of Wallonia - Belgium. Preprint at https://doi.org/10.1101/2020.08.29.20183210 (2020).
25. Aron, J., Giattino, C., Muellbauer, J. & Ritchie, H. A pandemic primer on excess mortality statistics and their comparability across countries. *Our World in Data* https://ourworldindata.org/covid-excess-mortality (2020).

# Article

## Methods

### Data reporting

No statistical methods were used to predetermine sample size. The experiments were not randomized and the investigators were not blinded to allocation during experiments and outcome assessment.

### Data

**Age- and sex-specific COVID-19-related fatality data.** We collated national-level age-stratified COVID-19-related death counts from official government and department of health webpages and reports for 45 countries. Where available, stratification by both age and sex was used. Subnational age-stratified death counts were additionally collated for four regions in which seroprevalence surveys had been conducted. For countries for which information on age was missing for a subset of deaths, we assumed the age distribution of the missing subset to be the same as that of the deaths with available age data. Information on age was missing for 29% of deaths in Spain. In addition, the time series of daily reported deaths from each country or region were obtained from the COVID-19 Data Repository by the Center for Systems Science and Engineering at Johns Hopkins University[26]. Age- and sex-specific population data were obtained from the United Nations 2019 World Population Prospects[27,28].

**Seroprevalence studies.** We used data from 25 SARS-CoV-2 seroprevalence surveys from 20 countries or regions for which the results were representative of the general population and for which age-stratified death data were also available; these results are shown in Fig. 1a and Supplementary Table 1. In the ensemble model, we consider only the 22 national-level seroprevalence surveys, which represent 16 countries. In cases in which estimates of seroprevalence reported by individual studies had not been adjusted for the performance of the seroprevalence assay, we used the reported values of assay sensitivity and specificity to adjust the reported seroprevalence values (Supplementary Table 1). Seroprevalence values from 24 out of 25 studies included in our analysis were adjusted for assay performance; the seroprevalence assay used by the one remaining study had not been reported at the time of publishing.

### Model

We combined age- and sex-specific COVID-19-related death data from 45 countries with data from 22 seroprevalence surveys, to jointly infer the age- and sex-specific IFRs and country-specific cumulative probabilities of infection. Age- and sex-specific IFRs were estimated in 5-year age groups, with individuals aged 80+ years considered as a single age group. Let $N_{c,a,s}$ be the population size for the age group $a$ of sex $s$ in country $c$. The expected number of deaths for the age group $a$ of sex $s$ in country $c$, $D_{c,a,s}$ is estimated as shown in equation (1), which we assume to follow a Poisson distribution. $\Lambda_c$ denotes the cumulative probability of infection in country $c$, $\delta_a$ the relative probability of infection in age group $a$ and $IFR_{a,s}$ the infection fatality ratio of age group $a$ and sex $s$. This assumes that age- and sex-specific IFRs are constant over the course of the pandemic. In cases in which improvements in COVID-19 outcomes have occurred over time, our estimates would represent the average probabilities to date.

$$D_{c,a,s} = N_{c,a,s} \Lambda_c \delta_a IFR_{a,s} \tag{1}$$

The expected number of deaths estimated by 5-year age groups were summed to match the corresponding age groups of observed deaths when reported in coarser age groups. We fit exclusively to the reported number of deaths for age groups under 65 years of age for each country (that is, including all age groups for which the upper bound is less than 65 years). IFRs for age groups aged 65 years and older were derived from age-specific death data reported by the Office for National Statistics in England[29], which allows us to exclude the age-specific number of deaths among residents of nursing homes (Supplementary Methods 2). As an external validation, we apply these IFRs to reported death data for a subset of 13 countries for which an adjustment for deaths that occurred in nursing homes could be applied (Supplementary Methods 2).

To align estimates of the cumulative probability of infection, $\Lambda_c$, with data from seroprevalence surveys, we used daily time series of reported deaths to infer the timing of infections and subsequent seroconversions. We assumed a gamma-distributed delay between onset and death[30] with a mean of 20 days and a standard deviation of 10 days and a gamma-distributed delay between infection and onset[31] with a mean of 6.5 days and standard deviation of 2.6 days. The delay between onset and seroconversion[32] was assumed to be gamma-distributed with a mean of 10 days and a standard deviation of 8 days. We derive the approximated seroprevalence at a given survey period $t$, $\lambda_{c,t}$, as shown in equation (2). Here, $S_{c,i}$ is the inferred number of seroconversions in country $c$ on day $i$, as inferred from the convolution of the death time series, $D_{c,i}$ is the number of new deaths reported in country $c$ on day $i$, and $T_c$ is the date of the reporting of the age-stratified cumulative death data.

$$\lambda_{c,t} = \Lambda_c \frac{\sum_{i=1}^{t} S_{c,i}}{\sum_{i=1}^{T_c} D_{c,i}} \tag{2}$$

We include all data from national-level seroprevalence studies in an ensemble model, in which the expected seroprevalence is assumed to follow a beta distribution with an unknown variance parameter, $\kappa$, as shown in equation (3). To investigate the contribution of different seroprevalence studies to the likelihood, the model was fitted separately to data from each individual seroprevalence survey, including an additional three subnational seroprevalence studies (Supplementary Table 1). For each seroprevalence survey, the expected number of seropositive individuals in country $c$ at sampling period $t$, $N_{c,t}^{positive}$, is assumed to follow a binomial distribution[33] as shown in equation (4), in which $N_{c,t}^{samples}$ is the number of serological samples taken in country $c$ at time $t$.

$$\overline{\lambda}_{c,t} \sim \text{beta}\left(\lambda_{c,t},\ \kappa\right), \tag{3}$$

$$N_{c,t}^{positive} \sim \text{binomial}\left(N_{c,t}^{samples},\ \lambda_{c,t}\right). \tag{4}$$

All parameters were estimated in a Bayesian framework using RStan[34] using R version 3.6.1. We assumed uniform priors on all parameters, between −50 and −0.001 on a logarithmic scale for all IFR estimates, and between −50 and 2 on a logarithmic scale for all estimates of the cumulative probability of infection. The model was run with 3 chains of 10,000 iterations each. The 95% credible intervals are calculated by taking the 0.025 and 0.975 quantiles of the posterior distribution.

### Reporting summary

Further information on research design is available in the Nature Research Reporting Summary linked to this paper.

### Data availability

Data are available at https://github.com/meganodris/International-COVID-IFR.

### Code availability

All code necessary to reproduce this analysis is available at https://github.com/meganodris/International-COVID-IFR.

26. Dong, E., Du, H. & Gardner, L. An interactive web-based dashboard to track COVID-19 in real time. *Lancet Infect. Dis.* **20**, 533–534 (2020).
27. De Wulf, M. *Population Pyramids of the World from 1950 to 2100.* https://www.population pyramid.net/world/2019/ (2016).

28. UN Department of Economic and Social Affairs. *World Population Prospects 2019*. https://population.un.org/wpp/ (UN, 2019).

29. Caul, S. Deaths registered weekly in England and Wales, provisional. https://www.ons.gov.uk/peoplepopulationandcommunity/birthsdeathsandmarriages/deaths/datasets/weeklyprovisionalfiguresondeathsregisteredinenglandandwales (UK Office for National Statistics, 2020).

30. Wu, J. T. et al. Estimating clinical severity of COVID-19 from the transmission dynamics in Wuhan, China. *Nat. Med.* **26**, 506–510 (2020).

31. Backer, J. A., Klinkenberg, D. & Wallinga, J. Incubation period of 2019 novel coronavirus (2019-nCoV) infections among travellers from Wuhan, China, 20–28 January 2020. *Euro Surveill.* **25**, 2000062 (2020).

32. Lou, B. et al. Serology characteristics of SARS-CoV-2 infection after exposure and post-symptom onset. *Eur. Respir. J.* **56**, 2000763 (2020).

33. Wu, J. T. et al. The infection attack rate and severity of 2009 pandemic H1N1 influenza in Hong Kong. *Clin. Infect. Dis.* **51**, 1184–1191 (2010).

34. Stan Development Team. RStan: the R interface to Stan. R package version 2 https://mc-stan.org/users/interfaces/rstan (2016).

**Author contributions** M.O., H.S. and S.C. conceived the study and performed the analysis. M.O., H.S., S.C., G.R.D.S., L.W. and J.P. collated data. G.R.D.S. and L.W. reviewed code. M.O., H.S. and S.C. wrote the first draft of the manuscript. M.O., H.S., S.C., G.R.D.S., L.W., D.A.T.C., A.S.A., J.P. and A.F. discussed the results and contributed to revisions of the manuscript.

**Competing interests** The authors declare no competing interests.

**Additional information**
**Supplementary information** is available for this paper at https://doi.org/10.1038/s41586-020-2918-0.
**Correspondence and requests for materials** should be addressed to M.O., S.C. or H.S.
**Peer review information** *Nature* thanks Gabriel Leung, Geert Molenberghs and the other, anonymous, reviewer(s) for their contribution to the peer review of this work. Peer reviewer reports are available.
**Reprints and permissions information** is available at http://www.nature.com/reprints.

# nature research

Corresponding author(s): Megan O'Driscoll

Last updated by author(s): Oct 19, 2020

# Reporting Summary

Nature Research wishes to improve the reproducibility of the work that we publish. This form provides structure for consistency and transparency in reporting. For further information on Nature Research policies, see our Editorial Policies and the Editorial Policy Checklist.

## Statistics

For all statistical analyses, confirm that the following items are present in the figure legend, table legend, main text, or Methods section.

| n/a | Confirmed | |
|---|---|---|
| ☐ | ☒ | The exact sample size ($n$) for each experimental group/condition, given as a discrete number and unit of measurement |
| ☐ | ☒ | A statement on whether measurements were taken from distinct samples or whether the same sample was measured repeatedly |
| ☒ | ☐ | The statistical test(s) used AND whether they are one- or two-sided *Only common tests should be described solely by name; describe more complex techniques in the Methods section.* |
| ☐ | ☒ | A description of all covariates tested |
| ☐ | ☒ | A description of any assumptions or corrections, such as tests of normality and adjustment for multiple comparisons |
| ☐ | ☒ | A full description of the statistical parameters including central tendency (e.g. means) or other basic estimates (e.g. regression coefficient) AND variation (e.g. standard deviation) or associated estimates of uncertainty (e.g. confidence intervals) |
| ☒ | ☐ | For null hypothesis testing, the test statistic (e.g. $F$, $t$, $r$) with confidence intervals, effect sizes, degrees of freedom and $P$ value noted *Give P values as exact values whenever suitable.* |
| ☐ | ☒ | For Bayesian analysis, information on the choice of priors and Markov chain Monte Carlo settings |
| ☐ | ☒ | For hierarchical and complex designs, identification of the appropriate level for tests and full reporting of outcomes |
| ☐ | ☒ | Estimates of effect sizes (e.g. Cohen's $d$, Pearson's $r$), indicating how they were calculated |

*Our web collection on statistics for biologists contains articles on many of the points above.*

## Software and code

Policy information about availability of computer code

| Data collection | No data collection software was used |
|---|---|
| Data analysis | R version 3.6.1 and RStan version 2.19.2 code available at https://github.com/meganodris/International-COVID-IFR |

For manuscripts utilizing custom algorithms or software that are central to the research but not yet described in published literature, software must be made available to editors and reviewers. We strongly encourage code deposition in a community repository (e.g. GitHub). See the Nature Research guidelines for submitting code & software for further information.

## Data

Policy information about availability of data

All manuscripts must include a data availability statement. This statement should provide the following information, where applicable:
- Accession codes, unique identifiers, or web links for publicly available datasets
- A list of figures that have associated raw data
- A description of any restrictions on data availability

All code and data necessary to reproduce the analyses are available from https://github.com/meganodris/International-COVID-IFR

# Field-specific reporting

Please select the one below that is the best fit for your research. If you are not sure, read the appropriate sections before making your selection.

☒ Life sciences ☐ Behavioural & social sciences ☐ Ecological, evolutionary & environmental sciences

For a reference copy of the document with all sections, see nature.com/documents/nr-reporting-summary-flat.pdf

# Life sciences study design

All studies must disclose on these points even when the disclosure is negative.

| | |
|---|---|
| Sample size | No sample sizes were calculated in this analysis |
| Data exclusions | No data were excluded |
| Replication | Co-authors reviewed code and verified the reproducibility of results |
| Randomization | N/A - the analysis does not involve experimental groups |
| Blinding | N/A - the analysis does not involve experimental groups |

# Reporting for specific materials, systems and methods

We require information from authors about some types of materials, experimental systems and methods used in many studies. Here, indicate whether each material, system or method listed is relevant to your study. If you are not sure if a list item applies to your research, read the appropriate section before selecting a response.

## Materials & experimental systems

| n/a | Involved in the study |
|---|---|
| ☒ ☐ | Antibodies |
| ☒ ☐ | Eukaryotic cell lines |
| ☒ ☐ | Palaeontology and archaeology |
| ☒ ☐ | Animals and other organisms |
| ☒ ☐ | Human research participants |
| ☒ ☐ | Clinical data |
| ☒ ☐ | Dual use research of concern |

## Methods

| n/a | Involved in the study |
|---|---|
| ☒ ☐ | ChIP-seq |
| ☒ ☐ | Flow cytometry |
| ☒ ☐ | MRI-based neuroimaging |